Int J Earth Sci (Geol Rundsch) (2006) 95: 225–238
DOI 10.1007/s00531-005-0030-1

ORIGINAL PAPER

Nassima Atmaoui · Nina Kukowski
Bernhard Stöckhert · Diethard König

Initiation and development of pull-apart basins with Riedel shear mechanism: insights from scaled clay experiments

Received: 30 April 2004 / Accepted: 1 June 2005 / Published online: 14 October 2005

Abstract Typical pull-apart structures were created in scaled clay experiments with a pure strike-slip geometry (Riedel type experiments). A clay slab represents the sedimentary cover above a strike-slip fault in the rigid basement. At an early stage of the development of the deformation zone, synthetic shear fractures (Riedel shears) within the clay slab display dilatational behaviour. With increasing basal displacement the Riedel shears rotate and open further, developing into long, narrow and deep troughs. The shear displacement and the low angle with the prescribed principal basal fault set them apart from tension gashes. At a more evolved stage, synthetic segments (Y-shears) parallel to the basal principal fault develop and accommodate progressive strike-slip deformation. The Y-shears connect the tips of adjacent troughs developed from the earlier Riedel shears, resulting in the typical rhomb-shaped structures characteristic for pull-apart basins. The Strait of Sicily rift zone, with major strike-slip systems being active from the Miocene to the Present, comprises pull-apart basins at different length scales, for which the structural record suggests development by a mechanism similar to that observed in our experiments.

Keywords Strike-slip faults · Pull-apart basins · Riedel shear · Analogue experiments · Clay models · Clay properties · Strait of Sicily rift zone

N. Atmaoui (✉) · B. Stöckhert
Institute for Geology, Mineralogy and Geophysics,
Ruhr-University Bochum, 44801 Bochum, Germany
E-mail: nassima.atmaoui@ruhr-uni-bochum.de

N. Kukowski
GeoForschungsZentrum Potsdam, 14473 Potsdam, Germany

D. König
Institute for Soil Mechanics and Foundation Engineering,
Ruhr-University Bochum, 44801 Bochum, Germany

Introduction

Pull-apart structures occur at different length scales (millimetre to plate boundary) in a wide range of tectonic settings. Typical pull-apart basins form in the sedimentary cover above strike-slip faults in the basement. The formation and accumulation of hydrocarbons renders these basins economically important—their structural evolution is of interest for oil and gas exploration.

Several mechanisms have been proposed for pull-apart basin formation. The most popular mechanism is local extension between two en echelon basement strike-slip fault segments (e.g. Aydin and Nur 1982; Mann et al. 1983). These can be right-stepping with dextral shear or left-stepping with sinistral shear. The local extension is accommodated in the sedimentary cover by normal faults at the releasing oversteps and bends (Fig. 1a). As alternatives, two other mechanisms have been proposed for the formation of pull-apart basins: a distributed (simple) strike-slip shear mechanism and a Riedel shear mechanism.

Distributed shear is envisaged to occur in weak layers of evaporites or overpressured shales, and above a broad strike-slip zone in the basement. This causes distributed shear deformation in the overlying competent sedimentary layers. Pull-apart basins can develop at releasing steps during fault interaction, coalescence and linkage (An and Sammis 1996 Fig. 1b).

The Riedel shear mechanism implies formation of pull-apart basins in the sedimentary cover along Riedel faults connected by segments of strike-slip faults, which are subparallel to a single principal displacement fault (PDZ) in the basement (Dewey 1978; Hagglauer-Ruppel 1991). The Riedel faults initiate first, while the strike-slip segments develop at a later stage and finally cause the formation of the pull-apart basins (Fig. 1c).

The development of pull-apart basins has been investigated theoretically (e.g. Rodgers 1980; Segall and Pollard 1980), numerically (e.g. Gölke et al. 1994; Katzman et al.

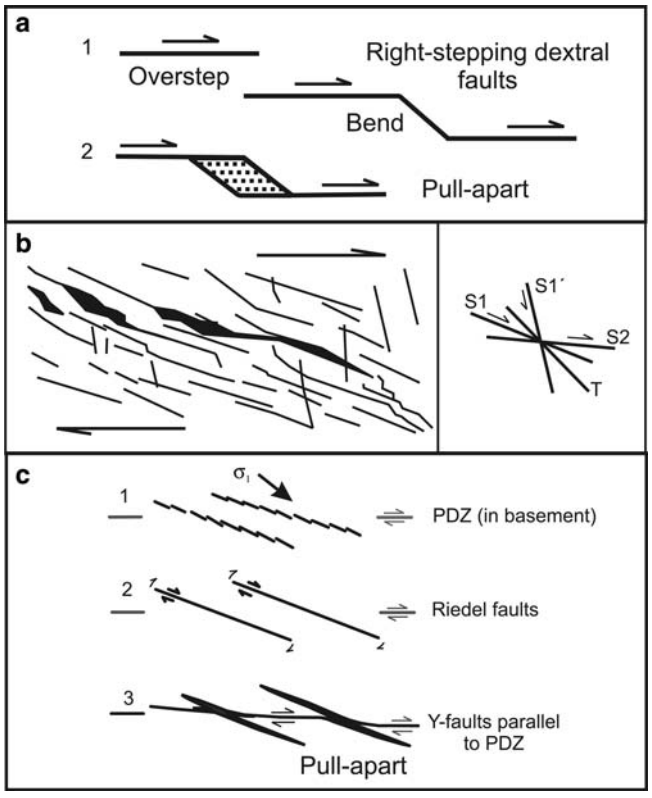

Fig. 1 Three mechanisms for the development of pull-apart basins. **a** En echelon right-stepping dextral strike-slip faults. Pull-apart basins form at the overstep or bend (Mirror image for the left-stepping sinistral faults). **b** Distributed shear. Pull-apart basins form during linking and coalescence of main faults. S_1 and $S_{1'}$ are primary synthetic and antithetic strike-slip faults, respectively. T and S_2 are tension and secondary synthetic strike-slip faults, respectively (simplified from An and Sammis 1996). **c** Riedel shear. *1* Initiation and coalescence of first generation shears into Riedel faults. *2* Strike-slip displacement and rotation of Riedel shears. *3* Development of Y-faults, parallel to the principal displacement zone (PDZ). Pull-apart basins form at the passive Riedel faults (modified from Hagglauer-Ruppel 1991)

1995), and experimentally for two en echelon strike-slip faults in the basement (e.g. Hempton and Neher 1986; McClay and Dooley 1995; Rahe et al. 1998). The experiments used a variety of set-ups and different materials. Synthetic and antithetic shears (referred to as Riedel and conjugate Riedel shears) and Y-shears were observed to develop in the laboratory experiments and are widespread in nature (e.g. Tchalenko 1970; Barlett et al. 1981; Gamond 1983; Gapais et al. 1991; Logan et al. 1992; Marone 1998; Schreurs 2003).

In this study we performed clay analogue experiments to study the formation of pull-apart basins by the Riedel shear mechanism. The aim is (1) to gain insight into the structural and kinematic evolution of pull-apart basins above a single strike-slip fault in the basement, and (2) to explore the influence of the shear strength of the clay and the thickness of the clay slab on the development of structures, with the perspective of appropriate scaling.

Previous analogue experiments on pull-apart basin formation

Here we give a short account of previous analogue experiments on the formation of pull-apart basins by one of the three principal mechanisms outlined above.

In en echelon strike-slip fault experiments the set-up consists of two straight basement discontinuities laterally offset to form a step-over of pre-determined geometry (set-up 1 in Fig. 2). The location and geometry of the modelled pull-apart structures are primarily controlled by the prescribed geometry in the basement (McClay and Dooley 1995; Le Calvez and Vendeville 2002).

The distributed strike-slip experiments are based on distributed flow in a weak layer (set-up 2 of Fig. 2). This can be simulated using a rubber or foam plastic sheet, or with sophisticated designs using multiple Plexiglas bars (Schreurs and Coletta 1998; Schreurs 2003) or multiple block units moving relative to each other in simple shear (Hoeppener et al. 1969). The experiments of An and Sammis (1996) were based on gravity sliding of a clay slab on a tilting board. In such experiments, the materials used to model the sedimentary cover are mainly clays (Cloos 1955; Hoeppener et al. 1969; An and Sammis 1996). The pull-apart structures observed by Cloos (1955) and Hoeppener et al. (1969) mainly originated along primary shear fractures, while those developed in the experiments of An and Sammis (1996) were bound by primary (s_1 or s_1') and secondary shear fractures or tension joints (s_2 and T; Fig. 1b).

The Riedel-type experiments simulate the transfer of deformation from a reactivated single and straight strike-slip fault in the basement into an overlying initially undeformed sedimentary cover. In the experiments, the single fault in the basement is simulated by two adjoining rigid plates, one of which can be moved parallel to the boundary in a dextral or sinistral manner (Cloos 1928; Riedel 1929, see set-up 3 of Fig. 2). Pull-apart structures bound by synthetic Riedel shears might have formed in the original clay experiments of Riedel, since he noted the opening of the synthetic shears at a later stage of deformation (Riedel 1929, p 363).

For this type of experiments, the properties of the material used for the simulation of the sedimentary cover are suspected to play a crucial role. In the wet clay experiments of Hagglauer-Ruppel (1991), very small pull-apart structures formed occasionally not only at the earliest small shear fractures, similar to the distributed shear experiments described above, but also at Riedel shears (Fig. 1c). Soula (1984) obtained similar results using sand and talc as analogue materials. The results of Soula (1984) and Hagglauer-Ruppel (1991) are significantly different from the Riedel type strike-slip experiments of earlier workers (e.g. Tchalenko 1970; Wilcox et al. 1973; Mandl 1988); possible reasons are discussed in a later section with respect to differences in material properties.

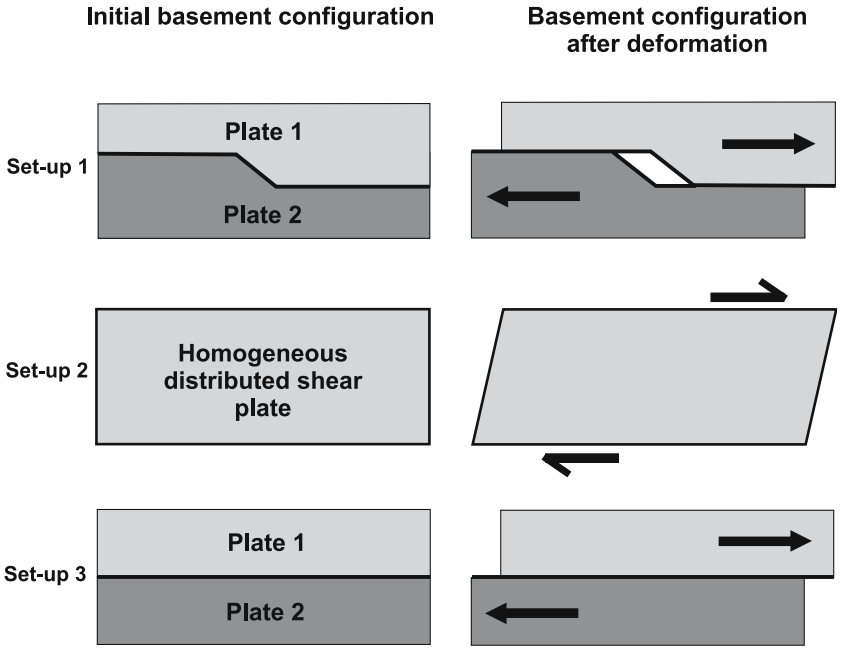

Fig. 2 Basement configuration of the three mechanisms in Fig. 1 before and after deformation. *Set-up 1* two offset discontinuities for the en echelon mechanism. *Set-up 2* simple shear of a basal plate for the distributed shear mechanism. *Set-up 3* one straight discontinuity for the Riedel shear mechanism

Mechanical properties of soft clay used in analogue experiments

Mechanical properties of clay

Laboratory constituted clays are excellent analogue materials to simulate brittle and ductile deformation in a sedimentary cover because of the following advantages:

(a) High deformability
(b) Brittle and ductile behaviour
(c) Wide range of variation in strength
(d) Delicate and persistent structural pattern.

Requirements (b) and (c) are mainly achieved through the variation of the water content of the clay pastes. For this purpose, the clay paste needs to be statistically isotropic and homogeneous, i.e. laboratory constituted and not an "as is" natural deposit.

In view of dynamic scaling laws, Cloos (1928) and Hubbert (1937) emphasised that the clay pastes appropriate for tectonic analogue experiments must be of extremely low shear strength, which can only be achieved at water contents at or beyond their Atterberg liquid limit (Whitlow 2001). The consistency of such clay pastes is simply inconvenient for soil mechanics and geotechnical laboratory testing, e.g. in direct shear or triaxial compression. So far no method is available to measure stresses and strains in extremely soft clays, loaded at very low effective stresses. Moreover, traditional soil mechanics had developed strength models for two basic classes of soils: sands being frictional and brittle, and clays being cohesive and ductile, neither being appropriate for the description of the clay pastes used in analogue modelling. Uncertainties on the notions of drainage condition (drained versus undrained) posed additional problems. Modern soil mechanics demonstrated that the traditional concepts to describe soil behaviour need to be replaced by new ones taking into account the state of the material and the boundary conditions (see below).

Here we first give a short outline of those aspects of clay behaviour, which are relevant in tectonic analogue experiments. For a background, the reader is referred to textbooks on basic soil mechanics concepts (e.g. Whitlow 2001), and on the critical state soil mechanics theory (Schofield and Wroth 1968; Atkinson and Bransby 1978; Wood 1990). To scale the clay experiments we need clays of extremely low shear strength and with a critical shear angle at failure similar to that of rocks in nature. In addition, we need to know the density of the clay paste at a specified water content. Physical and mechanical properties of the clay need to be determined at the state and at boundary conditions close to those used in the analogue experiments. Therefore a new procedure to determine the basic properties of modelling clays is introduced. It is based on routine tests performed in soil mechanics laboratories, on available correlations between the determined physical properties and the shear strength parameters, and on the material state (e.g. physical and mechanical properties, degree of saturation) and boundary conditions (e.g. drainage condition, stress ratio, type of performed test).

Physical state conditions in analogue modelling

Soil mechanics usually classifies clays into two categories: normally consolidated clays and overconsolidated clays. The consolidation state here refers to the stress history of a natural clay since deposition. The constituted clay is a mixture prepared in the laboratory, and

thus not subject to the typical process of consolidation. While a geoscientist would probably regard constituted clay as being in the unconsolidated state, it would be considered as normally consolidated in soil mechanics.

In scaled clay models, a clay–water mixture is prepared to obtain a very low shear strength, and a consistency which allows easy handling and preparation of clay slabs. Most clays display an extremely low shear strength at their liquid limit and beyond it (Atterberg's LL or W_L). At this state the clays are fully saturated or nearly so. Originally used for soil classification purposes, the Atterberg liquid (W_L or LL) and plastic limits (W_P or PL) are the bounding water contents between which the consistency of the soil is plastic. Consistency at this point is a physical state characteristic at a given water content. The range of plastic states is given by their difference and is termed plasticity index (I_P or PI). The Atterberg limits, determined with specific technical testing methods (Whitlow 2001), reflect the mineralogical characteristics of the clay size fraction.

The analogue experiments last up to 4 h. This time span is too short for a significant amount of water to be drained out or infiltrated during the experiment, which means that undrained conditions prevail.

Shear strength

Critical state soil mechanics (Schofield and Wroth 1968) provides a unified elastic–plastic model of soil behaviour. It should not be confused with the "critical state" in the critical taper theory (Davis et al. 1983; Dahlen et al. 1984), although both are based on the Coulomb failure criterion.

Mechanical tests show that the shear strength of clays depends primarily on the consolidation state. In the undrained condition, pore pressure increases in response to loading and becomes constant at the critical state while the volume is kept constant throughout shearing. At failure, there is a unique relationship between shear stress, normal stress, and volume (void ratio). A series of tests on normally consolidated clay will produce a critical state line passing through the origin ($\sigma' = 0$, $\tau_f = 0$):

$$\tau = \tau\prime = \sigma\prime \tan \phi_{cs}\prime = (\sigma - u) \tan \phi_{cs}\prime$$

where τ is the total shear stress at failure, τ' is the effective shear stress on the shear/slip surface at failure, σ' is the effective normal stress on the shear/slip surface at failure σ is the total normal stress on the shear/slip surface at failure, u is the fluid pressure acting on the slip surface at failure and ϕ_{cs}' is the angle of shear resistance at the critical state.

The rheological behaviour and the shear strength of the clay paste depend secondarily on the proportions of clay and other minerals, on the nature of the clay minerals, and on the water content. The shear strength of fine-grained soils is related to the plasticity index, the clay size fraction (CF; particles below 2 μm in diameter), and the nature of clay minerals. Volume changes or deformations occur by shear displacements or by sliding among particles or both (Sridharan 2002).

Dilatancy effects in normally consolidated clays are negligible to zero. Normally consolidated clays have no cohesion. The latter is explained in terms of an inadequate testing stress range, and any true cohesion in terms of effective stresses is either zero or very small (e.g. Bolton 1979; Santamarina 1997). The physical state of the material and the type of test used to determine the shear strength should match the conditions attained in the tectonic analogue experiments as close as possible.

Shear strength is best measured with a laboratory or a hand operated shear vane (Pilcon/Geonor™, used in this study). It is easy to handle and offers a direct reading dial. The determined values were found to compare well to those obtained in undrained triaxial compression results (e.g. Serota and Jangle 1972). The critical angle of friction ϕ_{cs}' is determined in triaxial compression tests. It is subject to technical problems caused by the extremely soft consistency of the modelling clay, however.

An empirical correlation between the plasticity index (I_P or PI) and the critical angle of friction (ϕ_{cs}') obtained in triaxial compression tests on normally consolidated clays (e.g. Ladd et al. 1977; Terzaghi et al. 1996) shows that the lower the plasticity index the higher is the critical angle of friction.

Based on the considerations above, silty clays and clays of the kaolinitic group with a low clay fraction (CF < 50%) are most suitable for the purpose of tectonic analogue modelling. They have a low to medium plasticity index (PI < 20%, and W_L < 40%) and their critical shear angle ϕ_{cs}' ranges between 29° and 38°.

Scaled clay models with Riedel shear mechanism

Material properties of the clay slabs

The material used to model the sedimentary cover in our strike-slip experiments is a silt-rich clay commercialised for ceramic purposes under the name "Kaolin-O". It is supplied by Erbslöh/Geisenheim Vertb., Germany, whose laboratories determined the mineralogical and chemical compositions. The clay minerals are kaolinite and illite. Quartz in the silt fraction makes up about 30% of the material. The physical and mechanical properties required for scaling have been determined at the soil mechanics laboratory of the Ruhr-University Bochum, Germany. The errors on the measurements are estimated to be less than ±2 on the last digit quoted in the tables; they are considered as insignificant for the present purpose.

Kaolin-O, a well graded silty clay, shows a wide distribution of particle sizes (from 1.5 to 55 μm), the clay size fraction CF being 41%. The Atterberg liquid and plastic limits of Kaolin-O are determined as 33% and 23%, respectively. The corresponding plasticity range is

Table 1 Undrained shear strength (S_u), bulk density (ρ_b), void ratio (e), and degree of saturation (Sr) corresponding to the water content of the clay pastes (w%) used in this study

water content (w%)	ρ_b (g/cm^3)	S_u (kPa)	e	Sr (%)
38	1.79	2	1.1	95
42	1.75	1.5	1.2	96
48	1.70	0.5	1.3	99

Note: water content is also termed moisture content or humidity in soil mechanics literature. It is the ratio of the weight of water contained in the pores to the weight of the solid dry material in a given mass of soil expressed as a percentage

relatively low (I_p = 10%). The shear strength of the clay pastes was varied by variation of the water content (w%). The bulk density, void ratio, degree of saturation, and the shear strength determined for the three materials used in our experiments, controlled by the water content (w = 38, 42 and 48%), are presented in Table 1.

Following critical state soil mechanics (Schofield and Wroth 1968), this clay is classified as normally consolidated clay; it has no cohesion intercept and fails at

$$\tau\prime = \sigma\prime \tan \phi_{cs}\prime$$

To derive the angle of internal friction ϕ_{cs}' from the plasticity index of the material we used the empirical correlation curve of Terzaghi et al. (1996), which was obtained from triaxial compression tests on normally consolidated clays. The plasticity index of 10% corresponds to $\phi_{cs}' = 32°$.

Scaling

Frictional sliding of mainly clastic sedimentary rocks at shallow depths ($z < 10$ km) may be described by a Mohr–Coulomb criterion, as discussed by Weijermars et al. (1993), where cohesion is taken as zero as in our model. In this case, the model to nature ratio of shear strength is as follows:

$$\tau* = \sigma * \tan \phi* = \rho * g * \lambda * \tan \phi*$$

where σ*, ρ*,g*, λ* and ϕ* are the model to nature ratios of normal stress, density, gravity, length and friction angle. Provided that the angle of internal friction of the modelling material corresponds to that of sedimentary rocks, this will send us back to the scaling law introduced by Hubbert (1937). Table 2 summarises the scaling properties of the used clays and of sedimentary rocks. With the experiments being performed in the same gravity field as in nature, 1 cm in the model corresponds to a length between 50 and 500 m in nature. A 4 cm thick clay slab is then equivalent to a 200–2000 m thick sedimentary cover.

Experimental set-up

The Riedel shear experiments were performed on a deformation table designed at the tectonic laboratory at the Ruhr-University Bochum (Brix et al. 1985). The motor-driven deformation table consists of two rigid plates, each 1 m long and 0.5 m wide. One of the plates is fixed to the frame of the apparatus, while the other is moved horizontally at a constant rate of 0.4 mm/min. The discontinuity between the plates simulates a dextral strike-slip fault in the basement, the pre-defined PDZ (Fig. 3). The long dimension of the clay slab can be extended up to 4 m with available accessories mounted on top of the deformation table. The amount of horizontal displacement is read from a fixed ruler, with a pointer connected to the moving plate. A wooden frame was used to fill the modelling material to the desired thickness (4 cm in the standard experiment), and to smoothen the upper surface of the slab. Passive circular markers were then drawn on the upper surface to visualise the deformation process and to allow displacement measurements.

Table 2 Properties of the modelling material and of sedimentary rocks with the scaling ratios.

	Sedimentary rocks	Model	Ratio
Bulk density (g/cm^3)	1.7–2.7	1.75	0.64–1
Shear strength (Pa)	[10–100]×10^6	1.5×10^3	2×10^{-4}–10^{-5}
Friction angle (°)	25–40	32	1

The experiments were performed to a maximum displacement of 83 mm. Photos taken at regular intervals document the progressive deformation and formed the basis for further analysis. In some experiments a digital video recorder was used. The cameras and the camcorder were mounted on a rail, which is fixed on the laboratory's ceiling just above the deformation table. The view is perpendicular to the upper surface of the slab. The dark lines seen on the plane view photos are strings extended a few centimetres above the surface and their corresponding shadow lines. They were added for the purpose of monitoring the vertical displacements generated along the shear zone; this aspect is not dealt with in the present paper. The scanned photos and digital images were analysed using an image analysis software (Core Image Analysis), which allows the measurement of properties such as length, area and angles.

In the present study, first a standard model with a clay slab of constant thickness (4 cm) and shear strength (1.5 kPa) was conducted. Then the parameters were varied in two series of experiments. In series (A) the shear strength of the clay slabs was varied, while the thickness was similar to the standard model. In series (B) the thickness of the clay slabs was varied while their shear strength remained unchanged.

Results

Standard experiment

The standard experiment produced a series of typical pull-apart structures in the model. Their progressive

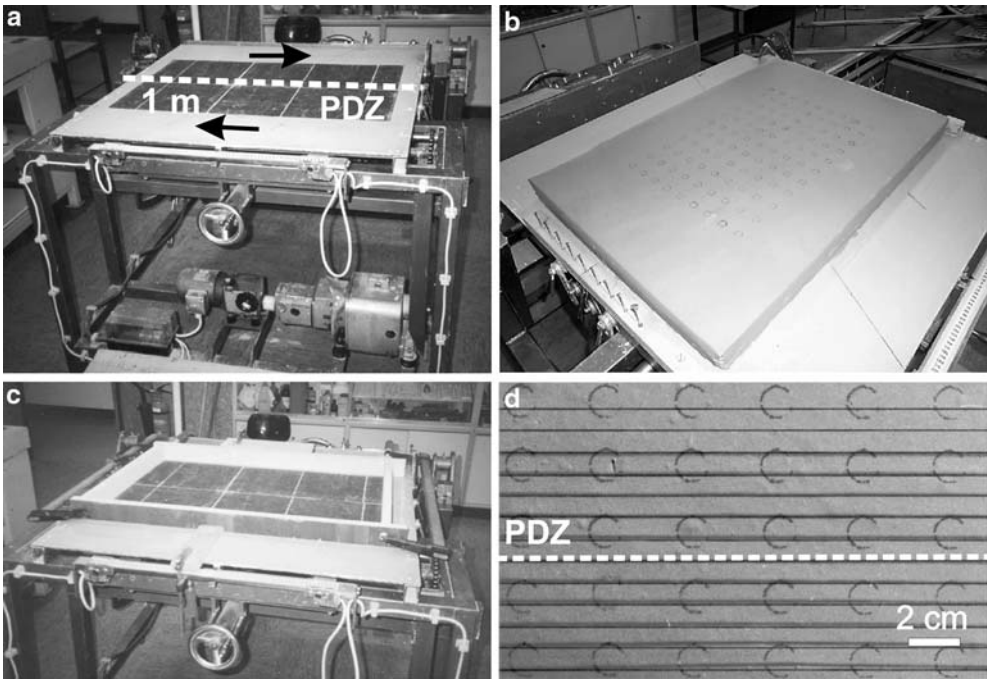

Fig. 3 Experimental set-up. **a** The deformation table. PDZ, a discontinuity between two rigid boards. **b** Installation of wooden frame for filling with clay and smoothing of surface. **c** Removal of wooden frame, extension of strings above the surface. **d** Plane view of the slab surface before deformation

development can be subdivided into three stages, depending on the horizontal basal displacement amount. In the present study the dextral basal displacement is normalised with respect to the thickness of the clay slab (NBD = normalised basal displacement), the width of the formed strike-slip zone in the model being dependent on the thickness of the slab.

The initial stage comprises the formation of Riedel shear fractures, as observed in other studies (e.g. Sylvester 1988). The first visible fractures appeared on the surface of the model after an NBD of 0.34 (i.e. after 1.36 cm of displacement). These first order fractures are of very small size (less than 1 mm), distributed along a deformation zone with a total width (or thickness) of about 6 cm at the surface and V-shaped in profile. Upon further displacement, these fractures coalesced to form en echelon left-stepping synthetic and antithetic shear fractures, in the following referred to as Riedel and conjugate Riedel shears. They became fully developed at an NBD of about 0.6. The lengths of the Riedel shears range between 2 and 8.8 cm, and their orientations vary between 8° and 23° to the principal basal displacement zone (Fig. 4a). Some of these Riedel shears display an extensional component, which here is a displacement normal to the shear direction. In the example shown in Fig. 4a, the Riedel shear fractures open by up to 14% of the amount of basal displacement, following a clockwise rotation by a few degrees. The presence of shear displacement as well as the small angle to the basal displacement zone distinguish them from the tension fractures, which are usually oriented at about 45° to the principal displacement zone and do not show any shear displacement. In the experiments by Cloos (1928) and Riedel (1929) tension fractures were observed to form only when water was sprayed on the surface of clay models.

The conjugate Riedel shears concentrate at the overstepping areas between the Riedel shears, with initial angles of orientation of 70–75° to the shear direction (Fig. 5). They show shear displacement and progressive rotation. They are observed to rotate 18–20° clockwise, while new ones developed at the initial angles. Rotation results in the characteristic 's′ shape. The conjugate Riedel shears serve to transfer the horizontal displacement from one Riedel shear to the adjacent one. They are not analysed further here, since they are not directly related to the formation of the pull-apart structures.

At an NBD of about 0.82 (i.e. D = 3.28 cm), Y- and sometimes P-shears initiate at some places along the strike-slip zone. These are synthetic shear fractures that are roughly parallel to the principal displacement zone (Fig. 4b). The Y-shears are regarded as the surficial segments paralleling the principal displacement zone. They preferentially form at the tips of the Riedel shears, rarely cutting through them, and accommodate the continuing strike-slip deformation while pulling the sides of the now passive Riedel shears further apart. Where the formation of the Y-shears was delayed, push-up structures developed instead at the restraining overstepping areas. Vertical displacement is expressed through the presence of a reverse component at the conjugate Riedel shears, and of small scale fold and thrust features.

Once the boundary Y- and P-shears were fully developed, the rhombic shape characterising the pull-apart basins is easily recognised (Fig. 4c). The angle of intersection between the two sets is below 30°. With further displacement two or more neighbouring structures can coalesce to form a long, narrow and deep complex or composite pull-apart basin (Fig. 4d).

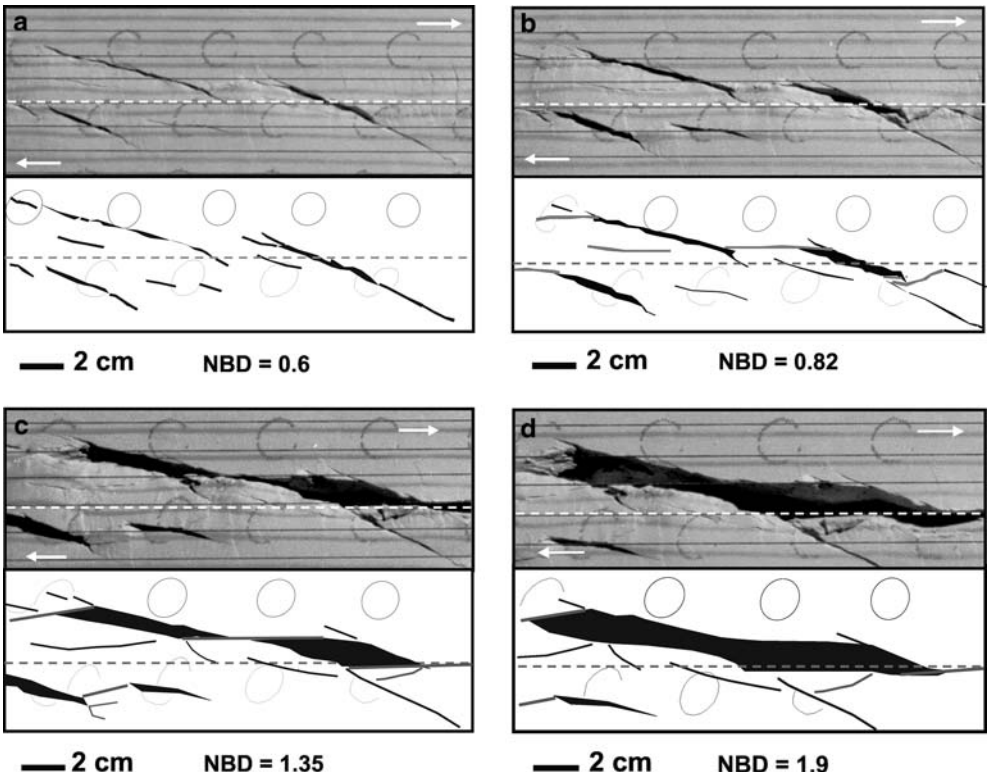

Fig. 4 Progressive development of pull-apart basins in standard experiment NA4 at normalised basal displacement magnitude (NBD). **a** Initiation and development of Riedel shears. **b** Initiation and development of the Y- and P-shears, incipient pull-apart structures. **c** Fully formed pull-apart structures at the Riedel shears. **d** Coalescence of neighbouring pull-apart structures. See text for more details

Influence of shear strength and thickness of the clay slab

The development of pull-apart structures at the Riedel shear fractures as described in the section above was observed in all experiments. The variation of the thickness and the shear strength of the clay slab was found to affect the width of the deformation zone and the number of shear fractures and pull-apart structures within the

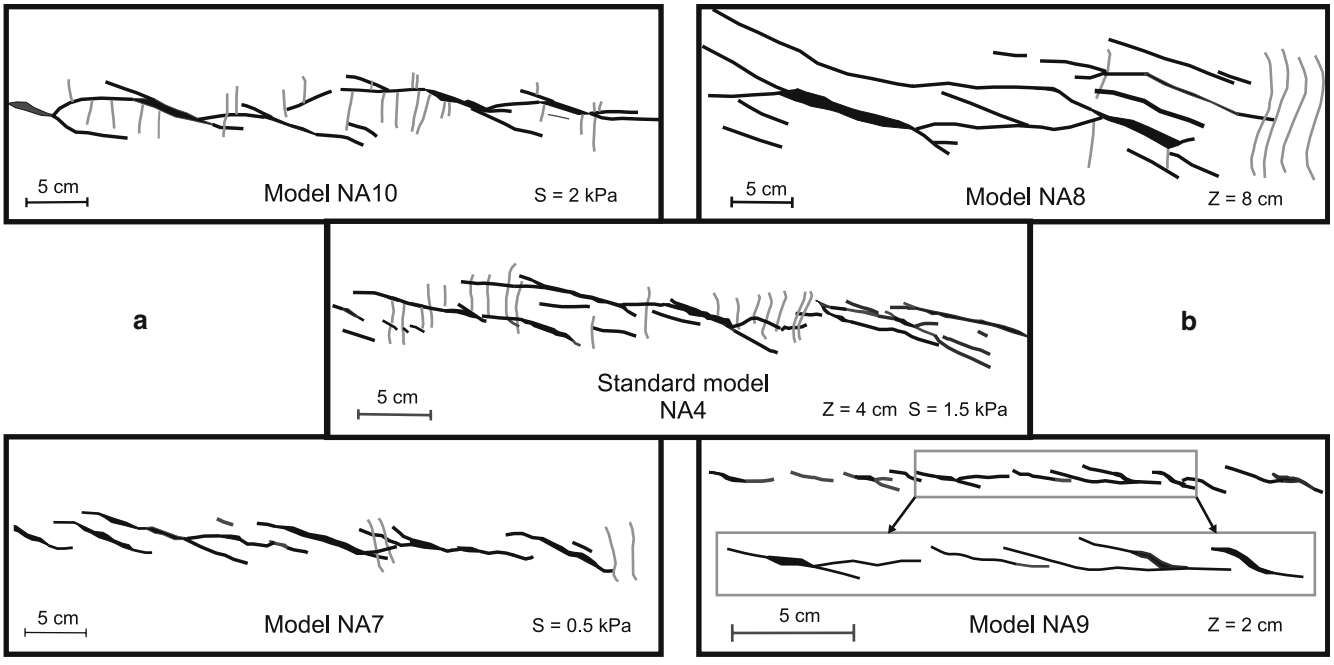

Fig. 5 Plane view of strike-slip deformation zones in various models by comparison to the standard model. Series (A): models of similar thickness (4 cm) and varying shear strengths. Series (B): models of similar shear strength (1.5 kPa) and varying thickness value. The structures are shown for a normalised basal shear displacement to thickness ratio of about 0.82. *Z* and *S* are, respectively, the thickness and the shear strength of the clay slab

Table 3 Influence of shear strength (S_u) and thickness (Z) of the clay slabs on the geometrical characteristics of deformation zones formed in the models

	NA4	NA7	NA8	NA9	NA10
Dimension (cm)	36×90	35×90	35×90	20×90	35×90
Thickness (cm)	4	4	8	2	4
Water content (%)	42	48	42	42	38
Undrained shear strength (kPa)	1.5	0.5	1.5	1.5	2
Displacement rate (mm/min)	0.41	0.44	0.43	0.42	0.40
Width of shear zone (cm)	5.2	4.1	11.5	2.2	5.7
Number of pull-apart structures	6	7	2	8	5
Average distance between pull-apart basins (cm)	9.7	3.9	13.2	4.4	9.1

deformation zones, counted for a slab length of 50 cm. These results are displayed visually in Fig. 5a, b, and in Table 3.

Influence of the shear strength (series A)

In series A clay slabs with water contents between 38 and 48% were used. This range corresponds to undrained shear strengths between 0.5 and 2 kPa. Even for relatively small differences in water content compared to the standard model (NA4 in Fig. 5a), significant variations in the deformation zone geometry were observed. First, the width of the shear zone increases with increasing shear strength for a constant thickness (Fig. 6; Table 3). Second, the experiment with low shear strength (NA7) shows only a few conjugate Riedel shears. These structures are much more frequent in the experiment with higher strength (NA10). Also, the number of Riedel shears increases with decreasing shear strength, and their spacing decreases accordingly (Fig. 5a, Table 3). Finally, the first shear fractures appear at the surface of the slab at a higher NBD when the shear strength of the clay is reduced. The first shear fractures appeared at an NBD of 0.38, 0.34 and 0.32 in models NA7, NA4 and NA10, respectively. The effect of shear strength is noticeable in Fig. 5a. At an NBD of about 0.82, the Y-shears are at an initial stage of development in model NA7, whereas they are already well developed at the same NBD in model NA10.

Influence of the thickness of the clay slab (series B)

The Riedel experiments of series B are characterised by a similar shear strength (1.5 kPa), and a variable thickness of the clay slab between 2 and 8 cm (Fig. 5b). The thickness of the clay slab turns out to control the width of the deformation zone, as shown in Table 3 and Fig. 6. The width of the strike-slip deformation zone is proportional to the thickness of the slab. Also, the number and the spatial distribution of the shear fractures formed within the deformation zone are strongly controlled by the thickness of the clay slab. For example, the conjugate Riedel shears are completely absent in the model with a clay slab thickness of 2 cm (NA9 in Fig. 5b). A minimum thickness of 4 cm is required for their development. Also, the number of Riedel shears per unit length is inversely proportional to the thickness of the clay slab (Table 3).

Figure 5b shows how these Riedel shears are distributed in space. The shear fractures developed in the en echelon pattern in all models, with a tendency for domains to overlap with increasing thickness of the clay slabs. They form a simple en echelon arrangement in model NA9 (2 cm thick), a mixed form of en echelon arrangement with domains of double- to triple-parallel traces in model NA4 (4 cm thick), and a more complex arrangement in model NA8 (8 cm thick). In this model 3–4 Riedel shears form domains with parallel traces. In this case, one of them is observed to become dominant and to develop into a pull-apart structure. Additionally, the greater the thickness of the clay slab, the larger is the amount of basal shear displacement required for the shears to appear at the surface. For an NBD of 0.82 as in Fig. 5b, the basal displacement D was 16, 33 and 64 mm in models NA4, NA9 and NA8, respectively.

Comparison with other analogue modelling studies

In this section the results of the present study are compared with previous Riedel type experimental studies. The specific properties of the Riedel type experiments are (1) the presence of a free upper surface (no vertical load is applied, and no general confinement), (2) the maximum principal stress is horizontal and not vertical as in the case of soil mechanics tests, and (3) the shear propagation and rotation is transferred from the basement to the upper surface. The latter property is referred to as basement induced wrenching by Mandl (1988). Distributed (simple) shear models and layered (upper crust/lower crust) models are not considered here.

Comparison with previous sand models

Our results are similar to those obtained by Soula (1984) in single layer models of fine-grained sand and talc powder. According to Soula (1984) the used sand and talc had a rather high cohesion, while Deramond et al. (1983) report the opposite. The physical and mechanical properties of the used materials are not described further by these authors.

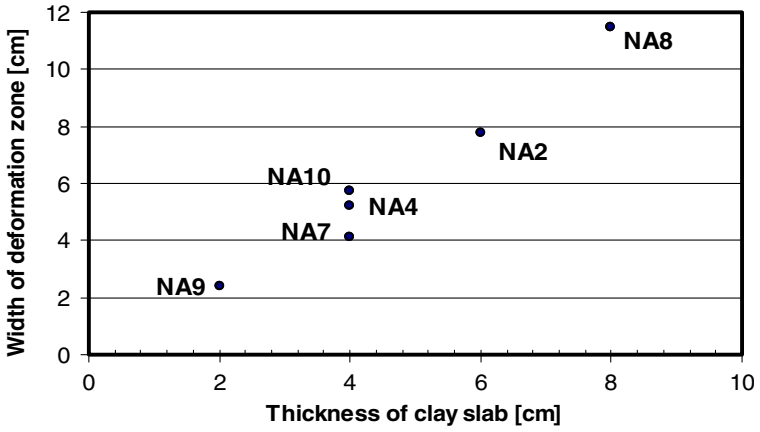

Fig. 6 The dependency of the width of the strike-slip zones on the thickness and the shear strength of the clay scaled models

Sandbox experiments dedicated to the influence of material properties on the development of strike-slip structures have been recently presented by Schöpfer and steyrer (2001). This study relies on a detailed specification of the physical and mechanical properties of used materials, which allows their comparison with other sandbox studies. Although similar in terms of cohesion and internal friction, sand and clay behave quite differently during deformation, which makes their comparison difficult. The differences are mainly related to the grain size distribution and grain shape, and to the behaviour of water in the pore space. Dry sand under stress deforms mainly by dilatancy and frictional flow (e.g. Schöpfer and Steyrer 2001), whereas hydro-physico-chemical effects at the interparticle contacts are important for clays (e.g. Ladd et al. 1977; Bolton 1979; Sridharan 2001). The clay particles are of platy shape, small size, and have electric charges in the presence of water. Wet clay under stress deforms by sliding along the long platy surfaces of the particles, strongly affected by pore pressure under undrained conditions.

Comparison with previous clay models

In contrast to sandbox experiments, the properties of the clays used for physical modelling are rarely specified, with the exception of Tchalenko (1970 and references to earlier work), and Lazarte and Bray (1996). Because clays show a wide range of behaviour at different states and conditions, it is very difficult to pinpoint which property or combination of properties might result in the opening of Riedel shear fractures. It is not clear, for instance, whether the plasticity index of the clay material is important, and what the influence of the mineral composition and the strength is.

The development of pull-apart structures presented in this study has not been described in the Riedel experiments of Tchalenko (1970) and Lazarte and Bray (1996). The plasticity index I_p of Kaolin-O used in our study is very low (10), whereas it was very high for the kaolinite–bentonite mixtures used by Lazarte and Bray (1996) (104 and 118, see Table 4). As described above in an earlier section, the plasticity index reflects the clay size fraction of the material and the nature of the minerals, and has a direct effect on the mechanical behaviour. The clay fraction of the kaolinitic clay used by Tchalenko (1970) was more than 95%. This might explain the absence of the opening of Riedel shears at the later stages of deformation. Also, the deformation rate might be of importance for the geometry of the failure structures. For the purpose of earthquake simulation experiments, Lazarte and Bray (1996) used high basal displacement rates (0.17–1.19 mm/s). They obtained smoothly curved surfaces in plane view and in profile. The marked V-shape was not observed. They noted that boundary conditions such as the model geometry and the presence or absence of boundary constraints (lateral confinement) and the material ductility (here referred to as plasticity) had a significant influence on the model response. Tchalenko (1970) concluded that continued research on the mechanisms of shear zone evolution should take into account other parameters.

Natural example of possible Riedel type pull-apart basins

Natural pull-apart basins that may have formed with the Riedel mechanism described in the present study are observed at different length scales on Gozo Island (Malta), which belongs to the Plio-Quaternary Strait of Sicily Complex rift zone. It is located on the eastern Pelagian platform of the Central Mediterranean, midway between Sicily and Tunisia. This WNW-ESE trending complex rift is about 380 km long and 100 km wide, and marks the boundary between the continental lithospheres of the African and the Eurasian plates. Its structure has been explored in geophysical studies, boreholes, and structural analyses carried out on the Pelagian islands and at Cap Bon in Tunisia. Details, interpretations and reviews of these different studies are given by Reuther (1980, 1990), Cello (1987), and Boccaletti et al. (1990).

Table 4 Comparison of material properties between different clays

Property	Tchalenko (1970)	Clays of Lazarte and Bray (1996)		Present study
Name and composition	Kaolin	Mix A kaolinite/bentonite	Mix B kaolinite/bentonite	Kaolin-O kaolin/silt
P_L and W_L	24–60	21–125	22–140	23–33
PI	36	104	118	10
Water content	45–56%	103–113%	112–118%	38–48%
Consolidation	Unknown	Normal		Normal
Shear strength	Unknown	Slightly above 2 kPa		0.5–2 kPa
CF	95%	Unknown		41%
Friction angle	23°	Unknown		32°

Sources: Tchalenko (1970), Morgenstern and Tchalenko (1967) and Lazarte and Bray (1996). P_L and W_L Atterberg's plastic and liquid limits; *PI* plasticity index or range; *CF* clay fraction with size below 2 μm

The continental crust in the strait of Sicily is about 20 km thick, and the sedimentary cover primarily consists of the Meso-Cenozoic platform carbonate series about 5 km thick. The Pantelleria, Malta, and Linosa basins are the major structural depressions associated with the complex rift zone (Fig. 7). They are 70–140 km long, and 15–30 km wide. The sedimentary filling of these basins consists of mainly Plio-Pleistocene turbidites, with an average thickness of 1–2 km, locally exceeding 3 km.

Most of the NW–SE to E–W trending bounding faults show oblique displacement with a significant dextral shear component. The post-Miocene remote stress field inferred from structural data, fault plane solutions and in-situ stress measurements is characterised by a NW–SE to NNW–SSE trending maximum horizontal stress. E–W to WNW–ESE trending transfer faults, which had developed during the Jurassic, were reactivated in the early Miocene as a result of dextral strike-slip motion between the African and the Eurasian plates (Morgan et al. 1998). The fault systems of the major depressions in the sedimentary cover began to develop in the late Miocene to early Pliocene. Deformation continues to the present day, related to ongoing extension and dextral displacement (Jongsma et al. 1985).

One of these E–W trending dextral strike-slip fault zones is located south of Gozo Island, where various stages of pull-apart basin development are observed on several length scales (Reuther 1980, 1990). A similar structural pattern was recently described by Kim et al. (2003) in the area north of Gozo Island, where pull-apart structures are developed along mesoscopic strike-slip zones. According to these studies, first-generation synthetic shears and faults (Riedel and conjugate Riedel shears) are formed, which are succeeded by extension fractures (Fig. 8). Reuther (1990) also described the reverse sequence. The faults occur on several length scales, with lengths ranging from centimetres to several hundreds of metres. Second-generation synthetic faults that are subparallel to the major fault zones (Y- and P-shears) link and pull the sides of the first-generation shears and extension fractures apart. It has been observed that the shape of the pull-apart structures formed from the Riedel shears was relatively long, narrow, and trapezoid, whereas the pull-apart structures formed from the extension fractures were wide trapezoids with higher intersection angle (Fig. 8a). Reuther (1980) observed that a horizontal clockwise rotation up to 20° is associated with the pull-apart structures of larger size, as well as formation of new Riedel shears and extension fractures. Plio-Quaternary pull-apart basins of kilometer-scale, formed by the mechanism described here, may be found offshore the Pelagian platform.

Discussion

The natural examples described above show that both extension fractures or normal faults and shear fractures or strike-slip faults can bound pull-apart structures formed along a strike-slip zone. Kim and Sanderson (2004) found that the strike-slip faults on Gozo Island shared many geometric features at different scales, the self similarity of the deformation zone structure being supported by a fractal analysis. The strike-slip zones in the Plio-Quaternary Strait of Sicily Complex rift zone are interpreted to be due to the reactivation of deep seated E–W to WNW–ESE trending faults, and due to fault propagation into the overlying sedimentary rocks. Assuming that the processes are similar to the Riedel type mechanism, the results of our experiments may help to understand their formation and evolution.

The first brittle structures that form in the clay models are the en echelon Riedel and conjugate Riedel shears. In the natural examples, this corresponds to the synthetic and antithetic strike-slip faults. No extension fractures were generated in our experiments, while earlier studies (e.g. Riedel 1929; Wilcox et al. 1973; Smith and Durney 1992) showed that such structures can appear at an early stage of deformation. The extension fractures and normal faults described by Reuther (1990) and Kim et al. (2003) also formed at an early stage. The Y- and P-shears formed at a later stage in our models correspond to the E–W trending synthetic faults in the natural examples. In this case the strike-slip motion is transferred to the E–W trending segments of the fault zone, pulling apart the previously formed synthetic and

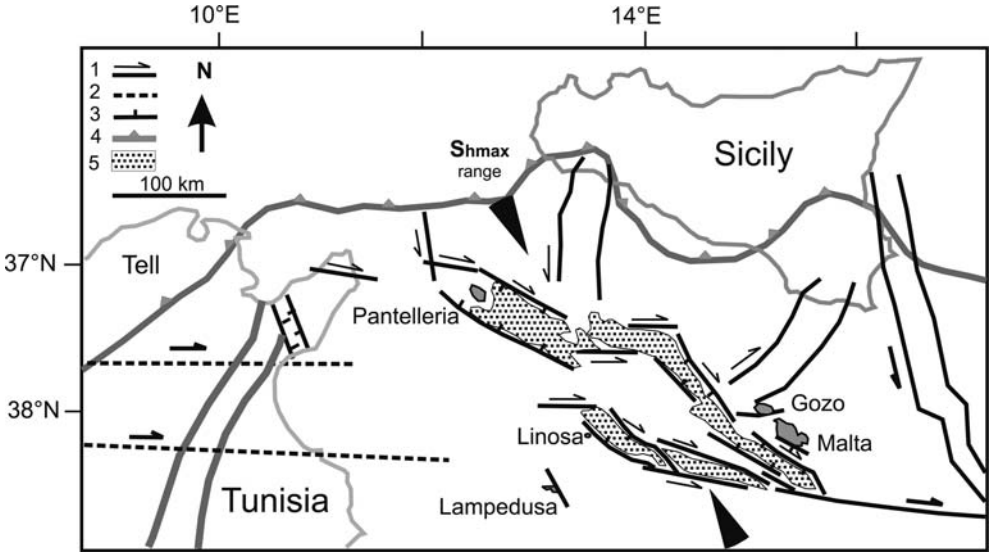

Fig. 7 The Strait of Sicily Complex rift zone. Modified after (Boccaletti et al. 1990 and Reuther 1990). *1* Strike-slip fault. *2* Deep basement fault. *3* Normal fault. *4* Thrusts and nappes front. *5* Plio-Quaternary basins

antithetic strike-slip and normal faults apart and creating the basins. This explains the major strike-slip component observed along the faults bounding the basins, as well as the small angle of about 22° (Fig. 8b) between the long axis of the basin and the E–W principal fault. For a bounding normal fault an angle close to 40° would be expected.

At a much larger scale, two models have been proposed for the evolution of the Plio-Quaternary Strait of Sicily Complex rift zone, both corresponding to the experimentally observed Riedel type mechanism. The differences between the two models are mainly due to differing assumptions on the orientation of the maximum horizontal stress: Reuther (1980, 1990) assumes σ_H to be oriented in a NW–SE direction, Cello (1987) and Boccaletti et al. (1990) assume a NNW–SSE direction. Both models neglect the strike-slip component observed along the bounding basins and their axial orientation.

The pull-apart structures produced in our present Riedel type experiments offer an alternative explanation, which is intermediate between the two proposed models. All the structural trends developed during the Pliocene to Quaternary tectonic activity within the Strait of Sicily Pelagian platform can be found in our model for σ_H oriented at about 45° to several E–W to WNW–ESE dextral principal displacement zones at depth. In this case the basin bounding faults, which show both normal and dextral displacement, are suggested to represent Riedel type strike-slip faults. In our dextral shear experiments, the Riedel shears initiated at angles between 8 and 23° to the principal displacement zone, but were affected by a clockwise rotation of up to 4°. The bounding oblique faults of the major basins of the Strait of Sicily Complex rift zone are mainly oriented at angles between 10 and 40° to the inferred principal E–W trending strike-slip faults at depth. This suggests that rotation of these structures may be more important than in the model. Reuther (1980) reports rotations by up to 20° in the pull-apart basins along the South Gozo fault.

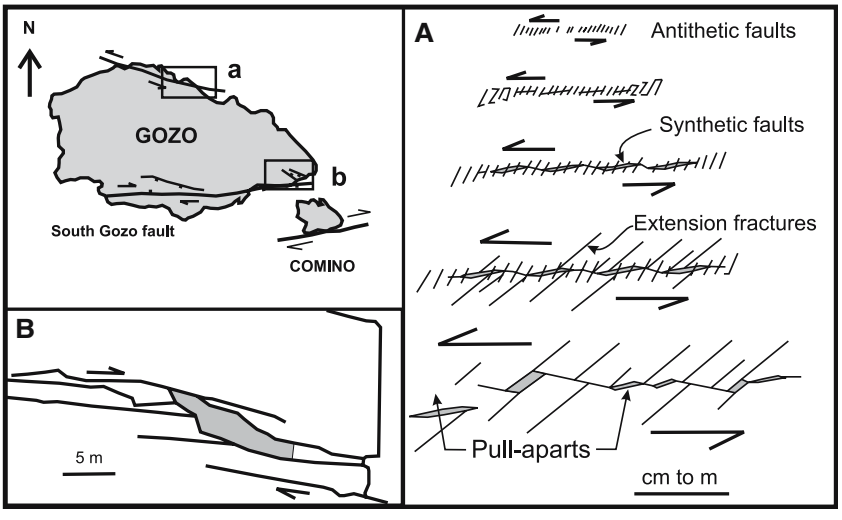

Fig. 8 Centimetre to several hundreds of metres long pull-aparts formed by the Riedel shear mechanism on Gozo, Malta **a** after Kim et al. (2003), **b** after Reuther (1990)

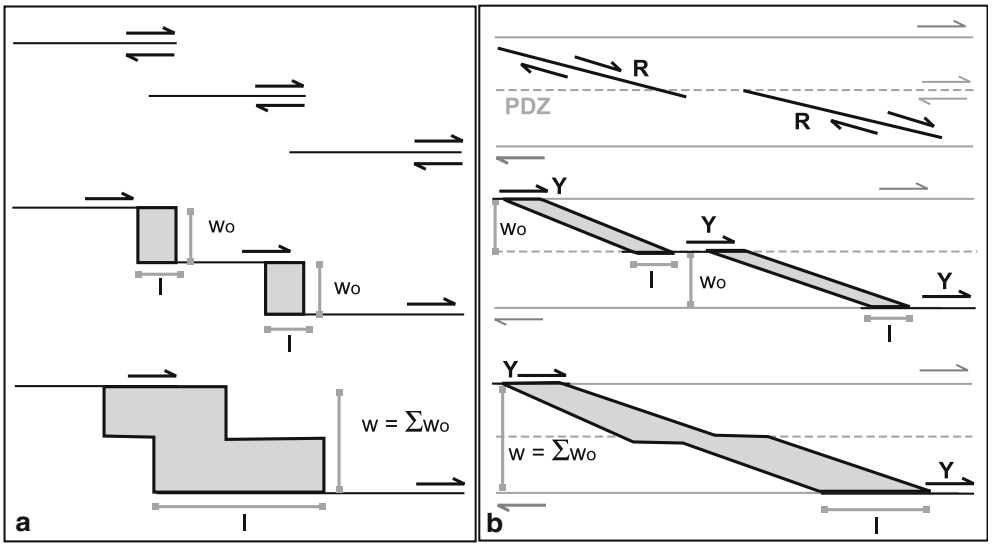

Fig. 9 Evolution of widths and lengths of pull-apart basins according to **a** Aydin and Nur (1982), and **b** the results of our clay analogue models. w_o Initial width of pull-apart basin; w width of coalesced pull-apart basin; l length of basin equal to fault offset; *PDZ* principal displacement zone; *R* Riedel shears/faults; *Y* shears/faults parallel to PDZ

Nilsen and Sylvester (1999) recognised six main types of strike-slip basins based on the geometry and kinematic setting, of which only the simple pull-apart type has been experimentally modelled so far. Also, many of the natural pull-apart basins may have a complex history. The different experimental set-ups used to model these basins are not contradictory (e.g. Hempton and Neher, 1986; McClay and Dooley, 1995; this study). They demonstrate several feasible mechanisms, one of which may be dominant at a certain stage or certain scale during the evolution of the basins. For natural pull-apart basins, the underlying Riedel mechanism can be identified from geological and geophysical field evidence. The main criteria are (1) presence of both a normal and a strike-slip component along the bounding faults of the incipient basins, (2) the relatively low angle between the oblique bounding faults and the principal strike-slip segments (below 30°), and (3) the high aspect ratio of the basins: with a long axis, a small width, and great depth.

The proposed evolution is close to the model of composite pull-apart basins proposed by Aydin and Nur (1982, their Model 1, Fig. 6 on p 99), where the length of the basin is equal to the offset at the bounding strike-slip faults, and the width of the basin is the sum of the widths of the initial pull-apart elements (Fig. 9a).

In the experiments, the length of the pull-apart structures, usually used to estimate the strike-slip offsets in nature, does not reflect the total horizontal displacement along the basal deformation zone. The reason is that the initial Riedel shear fractures which bound the developing pull-apart structures accommodated a significant amount of the basal displacement prior to the formation of the basins (Fig. 9b).

In all three mechanisms introduced in the first chapter, the displacement along the basal fault is important, since the formation of pull-apart basins commences only after the development of the Y- and P-segments. In contrast, models based on the en echelon basement strike-slip fault type mechanism show that step-over geometry in the basement is a primary factor controlling the location and geometry of the pull-apart structures.

During the processes that lead from original sediment deposition to the formation of consolidated rocks, material properties of the sediments and sedimentary rocks undergo significant changes. Our scaled analogue experiments have shown that material properties distinctly influence the development and geometry of pull-apart basins forming above a basement strike-slip fault. This infers that in nature the processes of pull-apart basin formation may differ if they take place in sedimentary rocks of different stages of consolidation. Therefore it might be crucial for understanding pull-apart basin formation in nature to know the exact timing and history of basin evolution relative to related tectonic and depositional processes. Such an effort is only possible if geophysical structural imaging, structural geological field work, and laboratory experimental modelling are conducted in close relation.

Conclusions

The Riedel mechanism of pull-apart formation is investigated in scaled analogue experiments with clay slabs of variable thickness and shear strength representing the sedimentary cover. The shear strength (controlled by the water content) and the thickness control the width of the deformation zone, the number and spacing of the Riedel shears, the presence or absence of the conjugate Riedel shears and the amount of basal shear displacement required for the shear fractures to appear at the surface. The dependencies can be summarised as follows:

1. The width of the strike-slip deformation zone increases with increasing shear strength and with increasing thickness of the clay slab.

2. The number of conjugate Riedel shears increases with increasing shear strength. A minimum thickness of 4 cm (corresponding to 0.2–2 km in nature) is required for their development.
3. The number of Riedel shears increases with decreasing shear strength, and their spacing decreases accordingly. Also, the number of Riedel shears per unit length is inversely proportional to the thickness of the clay slab.
4. The shear fractures developed in an en echelon pattern in all models, with a tendency for more complex arrangement with increasing thickness of the clay slab.
5. The amount of basal shear displacement required for the first shears to appear at the surface increases with decreasing shear strength and increasing thickness of the clay slab.

In order to scale such models, clays of extremely low shear strength and with a critical shear angle at failure similar to that of sedimentary rocks are needed. In addition, we need to know the density of the clay at a particular water content. It is important that the physical and mechanical properties of the clays are determined at the state and boundary conditions corresponding to those attained in the tectonic analogue experiments. Clays that fulfill the above criteria are nearly saturated silty clays and clays of the kaolinitic group, deformed under undrained conditions at very low effective stresses. Such clays are characterised by a low clay fraction (CF $<$ 50%), a low to medium plasticity index (PI $<$ 20%, and W_L $<$ 40%), and an angle of internal friction ϕ_{cs}' between 29 and 38°.

In the experiments, the length of the pull-apart structures, usually used to estimate the strike-slip offsets in nature, does not reflect the total horizontal displacement in the basement. The initial Riedel shear fractures bounding the developing pull-apart structures accommodated a significant amount of the basal displacement prior to the formation of the basins. The close correspondence between the experimental results and the natural examples of pull-apart basins in the Strait of Sicily Rift suggests that the mechanisms of basin formation may be scale-independent.

Acknowledgements We wish to thank the DAAD (Deutscher Akademischer Austausch Dienst) for awarding a research scholarship to N.A.. Our sincere thanks go to Prof. H.-U. Schwarz for the invaluable introduction to the tectonic laboratory of the Geology, Mineralogy and Geophysics institute at the Ruhr-University. We are also grateful to J. Lohrmann, A. Adriasola, and J. Steffahn for extensive discussions and comments. We thank G. Schreurs and an anonymous reviewer for their constructive comments on an earlier version of the manuscript.

References

An L-J, Sammis CG (1996) Development of strike-slip faults: shear experiments in granular materials and clay using a new technique. J Struct Geol 18:1061–1077

Atkinson JH, Bransby PL (1978) The mechanics of soils: an introduction to critical state soil mechanics. McGraw-Hill, London, pp 1–375

Aydin A, Nur A (1982) Evolution of pull-apart basins and their scale independence. Tectonics 1:91–105

Barlett WL, Friedman M, Logan JM (1981) Experimental folding and faulting of rocks under confining pressure. Tectonophysics 79:255–277

Boccaletti M, Cello G, Tortorici L (1990) Strike-slip deformation as a fundamental process during the Neogene-Quaternary evolution of the Tunisian-Pelagian area. Ann Tecton Special issue 4:104–119

Bolton M (1979) A guide to soil mechanics. Macmillan Press, London, pp 1–439

Brix M, Schwarz H-U, Vollbrecht A (1985) Tektonische Experimente als Beitrag zu Strukturanalysen im Ruhrkarbon. Glückauf-Forschungshefte 46(H.4):192–199

Cello G (1987) Structure and deformation processes in the Strait of Sicily "rift zone". Tectonophysics 141:237–247

Cloos H (1928) Experimente zur inneren Tektonik. Centralbl Mineral Pal 5:609–621

Cloos E (1955) Experimental analysis of fracture patterns. Geol Soc Am Bull 66:241–256

Dahlen FA, Suppe J, Davis D (1984) Mechanics of fold-and-thrust belts and accretionary wedges: cohesive Coulomb theory. J Geophys Res 89:10087–10101

Davis D, Suppe J, Dahlen FA (1983) Mechanics of fold-and-thrust belts and accretionary wedges. J Geophys Res 88:1153–1172

Deramond J, Sirieys P, Soula JC (1983) Mécanismes de déformation de l'écorce terrestre: structures et anisotropie induites. In: 5th congress international Society Rock Mechanism Melbourne F:89–93

Dewey JF (1978) Origin of long transform-short ridge systems. Geol Soc America 10:388

Gamond J-F (1983) Displacement features associated with fault zones: a comparison between observed examples and experimental models. J Struct Geol 5:33–45

Gapais D, Fiquet G, Cobbold PR (1991) Slip system domains, 3. New insights in fault kinematics from plane-strain sandbox experiments. Tectonophysics 188:143–157

Gölke M, Cloetingh S, Fuchs K (1994) Finite-element modelling of pull-apart basin formation. Tectonophysics 240:45–58

Hempton M, Neher K (1986) Experimental fracture, strain and subsidence patterns over en echelon strike-slip faults: implications for the structural evolution of pull-apart basins. J Struct Geol 8:597–605

Hoeppener R, Kalthoff E, Schrader P (1969) Zur physikalischen Tektonik. Bruchbildung bei verschiedenen affinen Deformationen im Experiment. Geol Rdsch 59:179–193

Hubbert MK (1937) Theory of scale models as applied to study of geological structures. Geol Soc Am Bull 48:1459–1520

Jongsma D, van Hinte JE, Woodside JM (1985) Geologic structure and neotectonics of the North African Continental Margin south of Sicily. Marine Petrole Geol 2:156–179

Katzman R, ten Brink US, Lin J (1995) 3-D modelling of pull-apart basins: Implications for the tectonics of the Dead Sea Basin. J Geophys Res 100:6295–6312

Kim Y-S, Sanderson D (2004) Similarities between strike-slip faults at different scales and a simple age determining method for active faults. Island-Arc 13:128–143

Kim Y-S, Peacock DCP, Sanderson D (2003) Mesoscale strike-slip faults and damage zones at Marsalforn, Gozo Island, Malta. J Struct Geol 25:793–812

Ladd CC, Foott R, Ishihara K, Schlosser F, Poulos HG (1977) Stress-deformation and strength characteristics. Proc 9th International Conference on soil mechanics and foundation engineering, Tokyo 2:421–482

Lazarte CA, Bray JD (1996) A study of strike-slip faulting using small-scale models. Geotech Testing J 19:118–129

Le Calvez JH, Vendeville BC (2002) Experimental designs to model along-strike fault interaction. In: Schellart WP, Passchier

C (eds) Analogue modelling of large-scale tectonic processes. J Virtual Explorer 7:7–23
Logan JM, Dengo CA, Higgs NG, Wang ZZ (1992) Fabrics of experimental fault zones: their development and relationship to mechanical behaviour. In: Evans B, Wong T-F (eds) Fault mechanics and transport properties of rocks. Academic, London, pp 33–67
Mandl G (1988) Mechanics of tectonic faulting. Elsevier, Amsterdam, pp 135–152
Mann P, Hempton MR, Bradley DC, Burke K (1983) Development of pull-apart basins. J Geol 91:529–554
Marone C (1998) Laboratory-derived friction laws and their application to seismic faulting. Ann Rev Earth Planet Sci 26:643–696
McClay K, Dooley T (1995) Analogue models of pull-apart basins. Geology 23:711–714
Morgan MA, Grocott J, Moody RTJ (1998) The structural evolution of the Zaghouan-Ressas Structural Belt, northern Tunisia. In: Macgregor DS, Moody RTJ, Clark-Lowes DD (eds.). Petroleum geology of North Africa: Geol Soc London, Spec Publ 132:405–422
Morgenstern NR, Tchalenko JS (1967) Microscopic structures in kaolin subjected to direct shear. Geotechnique 17:309–328
Nilsen TH, Sylvester AG (1999) Strike-slip basins. Part 1. The Leading Edge 18:1146–1152
Rahe B, Ferill DA, Morri AP (1998) Physical analogue modelling of pull-apart basin evolution. Tectonophysics 285:21–40
Reuther C-D (1980) Das Pantelleria Rift. Kinematik miozäner bis rezenter Krustendehnungsprozesse bei Konvergenter Intraplattentektonik im zentralen Mittelmeer. Habilitation manuscript, Fridericiana University of Karlsruhe, Germany, pp 1–139
Reuther C-D (1990) Strike-slip generated rifting and recent tectonic stresses on the African foreland (Central Mediterranean region). Ann Tecton Spec issue 4:120–130
Riedel W (1929) Zur mechanik geologischer Brucherscheinungen. Zentralblatt Mineral Geol Paläont B:354–368
Rodgers DA (1980) Analysis of pull-apart basin development produced by en-echelon strike-slip faults. Int Assoc Sedimentol Spec Publ 4:27–41
Santamarina JC (1997) ''Cohesive soils'': a dangerous oxymoron. Electronic Journal of Geotechnical Engineering, iGEM Magazine
Schofield AN, Wroth CP (1968) Critical state soil mechanics. McGraw-Hill, London
Schöpfer MPJ, Steyrer HP (2001) Experimental modelling of strike-slip faults and the self-similar behaviour. In: Koyi HA, Mancktelow NS (eds) Tectonic Modeling. A volume in honor of Hans Ramberg. Geol Soc Am Memoir 193:21–27
Schreurs G (2003) Fault development and interaction in distributed strike-slip shear zones: an experimental approach. In: Storti F, Holdsworth RE, Salvini F (eds) Intraplate strike-slip deformation belts. Geol Soc London Spec Publ 210:35–52
Segall P, Pollard D (1980) Mechanics of discontinuous faults. J Geophys Res 85:4337–4350
Serota S, Jangle A (1972) A direct-reading pocket shear vane. Civil Eng ASCE 42:73–76
Smith JV, Durney DW (1992) Experimental formation of structural assemblages in oblique divergence. Tectonophysics 216:235–253
Soula J-C (1984) Genese de basins sédimentaires en régime de cisaillement transcurrent: modèles expérimentaux et exemples géologiques. Bull Soc Belge Géol 93(1–2):83–104
Sridharan A (2002) Engineering behaviour of clays: influence of mineralogy. In: Di Maio C, Hueckel T, Loret B (eds) Chemo-mechanical coupling in clays: from nano-scale to engineering applications. Swets and Zeitlinger, Lisse, pp 3–28
Sylvester AG (1988) Strike-slip faults. Geol Soc Am Bull 100:1666–1703
Tchalenko JS (1970) Similarities between shear zones of different magnitudes. Geol Soc Am Bull 81:1625–1640
Terzaghi K, Peck RB, Mesri G (1996) Soil mechanics in engineering practice. Wiley, New York, pp 1–208
Weijermars R, Jackson MPA, Vendeville BC (1993) Rheological and tectonic modelling of salt provinces. Tectonophysics 217:143–174
Whitlow R (2001) Basic soil mechanics. Pearson Education Ltd, London, pp 1–571
Wilcox RE, Harding TP, Seely DR (1973) Basic wrench tectonics. Am Assoc Petr Geol Bull 57:74–96
Wood MD (1990) Soil behaviour and critical soil mechanics. Cambridge University Press, Cambridge